Journal of Cellular Biochemistry 98:1320–1333 (2006)

The Exonuclease ISG20 Mainly Localizes in the Nucleolus and the Cajal (Coiled) Bodies and Is Associated With Nuclear SMN Protein-Containing Complexes

Lucile Espert,[1] Patrick Eldin,[1] Céline Gongora,[1] Bernard Bayard,[1] Francis Harper,[3] Mounira K. Chelbi-Alix,[2] Edouard Bertrand,[4] Geneviève Degols,[1] and Nadir Mechti[1]*

[1]UMR5160 CNRS, EFS, 240 avenue Emile Jeanbrau, 34094 Montpellier Cedex 5, France
[2]UPR9045 CNRS, Institut André Lwoff, 7 Rue Guy Moquet, 94801 Villejuif, France
[3]UPR1983 CNRS, Institut André Lwoff, 7 Rue Guy Moquet, 94801 Villejuif, France
[4]IGMM CNRS, 1919 route de Mende, 34095 Montpellier Cedex 5, France

Abstract We have previously shown that ISG20, an interferon (IFN)-induced gene, encodes a 3′ to 5′ exoribonuclease member of the DEDD superfamily of exonucleases. ISG20 specifically degrades single-stranded RNA. In this report, using immunofluorescence analysis, we demonstrate that in addition to a diffuse cytoplasmic and nucleoplasmic localization, the endogenous ISG20 protein was present in the nucleus both in the nucleolus and in the Cajal bodies (CBs). In addition, we show that the ectopic expression of the CBs signature protein, coilin, fused to the red fluorescent protein (coilin-dsRed) increased the number of nuclear dots containing both ISG20 and coilin-dsRed. Using electron microcopy analysis, ISG20 appeared principally concentrated in the dense fibrillar component of the nucleolus, the major site for rRNA processing. We also present evidences that ISG20 was associated with Survival of Motor Neuron (SMN)-containing macromolecular nuclear complexes required for the biogenesis of various small nuclear ribonucleoproteins. Finally, we demonstrate that ISG20 was associated with U1 and U2 snRNAs, and U3 snoRNA. The accumulation of ISG20 in the CBs after IFN treatment strongly suggests its involvement in a new route for IFN-mediated inhibition of protein synthesis by modulating snRNA and rRNA maturation. J. Cell. Biochem. 98: 1320–1333, 2006.

Key words: ISG20; interferon; exonuclease; Cajal bodies; SMN

The processing and turnover of the different classes of RNA require the action of a large number of ribonucleases (RNase), including endo and exoribonucleases [Beelman and Parker, 1995; Deutscher and Li, 2001; Tourriere et al., 2002]. Extensive sequence and catalytic properties analysis have allowed to group the exoribonucleases into six main superfamilies, RNR, DEDD, RBN, PDX, RRP4, and 5PX and a variety of subfamilies [Moser et al., 1997; Zuo and Deutscher, 2001]. In particular, DEDD is a large exonuclease superfamily, which includes RNases such as RNase T and D, the proofreading domains of the Pol I family of DNA polymerases, and other DNA exonucleases. Homologies within this superfamily are concentrated at three separate conserved exonuclease motifs termed ExoI, ExoII, and ExoIII with four invariant acidic amino acids (D: aspartic acid, E: glutamic acid) and several other conserved residues [Moser et al., 1997; Zuo and Deutscher, 2001]. Members of this superfamily can have both RNase and DNase activities. Based on these alignment studies, ISG20, an interferon (IFN)-inducible protein, was shown to be a member of the DEDD family [Gongora et al., 1997; Moser

Lucile Espert and Patrick Eldin have contributed equally to the study.

Grant sponsor: Association pour la Recherche contre le Cancer and the Centre National de la Recherche Scientifique.

*Correspondence to: Nadir Mechti, UMR CNRS 5160, EFS, 240 Avenue Emile Jeanbrau, 34094 Montpellier Cedex 5, France. E-mail: nadir.mechti@cpbs.univ-montp1.fr

Received 24 October 2005; Accepted 20 January 2006
DOI 10.1002/jcb.20869

et al., 1997]. Biochemical analysis allowed us to identify ISG20 as a 3′ to 5′ exonuclease specific for single-stranded RNA and, to a lesser extent, DNA [Nguyen et al., 2001]. A single substitution of a conserved aspartic acid by a glycine residue is sufficient to abolish its exonuclease activity [Nguyen et al., 2001]. Amino acid comparison suggests that ISG20 might be a human homolog of the yeast protein Rex4p, member of the Rex DEDD subfamily [van Hoof et al., 2000]. Interestingly, various Rex proteins have been shown to have a unique and overlapping function in the processing of many RNA species, including 5S and 5.8S rRNAs, U4, and U5 small RNAs (snRNAs), RNase MPR, and RNase P RNAs [van Hoof et al., 2000]. Even though the exact specificity of Rex4p fails to be determined, these data suggest that ISG20 might be involved in the processing of rRNA, snRNAs, or components required for ribosome biogenesis.

In mammalian cells, these processes mainly occur in discrete and dynamic nuclear structures named the nucleolus and the Cajal bodies (CBs) [Lamond and Earnshaw, 1998; Gall, 2000; Dundr and Misteli, 2002; Carmo-Fonseca, 2002a]. The nucleoli are organized around rRNA gene clusters and they are considered as the center of rRNA processing and ribosome subunit biogenesis [Shaw and Jordan, 1995; Lamond and Earnshaw, 1998; Scheer and Hock, 1999; Olson et al., 2000; Dundr and Misteli, 2001]. However, they are now also clearly involved in the maturation of non-ribosomal RNA species [Kadowaki et al., 1995; Schneiter et al., 1995; Pederson, 1998]. The CBs are non-membrane-bound nuclear suborganelles implicated in the post-transcriptional maturation of small nuclear (snRNAs) and small nucleolar (snoRNAs) RNAs [Samarsky et al., 1998; Matera, 1999; Narayanan et al., 1999; Verheggen et al., 2002; Jady et al., 2003; Sleeman et al., 2003]. At the physiological level, the CBs vary in number and size among cell types and also show cell cycle variation [Ogg and Lamond, 2002; Carmo-Fonseca, 2002b]. Their presence in the cells is the marker of active transcriptional processes [Gall et al., 1999; Gall, 2000; Gall, 2001; Ogg and Lamond, 2002]. Now, it is clear that the CBs and the nucleolus are highly mobile compartments responding to the cellular environment and functionally interacting together. Indeed, prior to their processing by endo and exonucleases, the rRNAs require post-transcriptional modifications directed by snoRNAs that are themselves processed in the CBs before being imported to the nucleoli [Tollervey and Kiss, 1997; Scheer and Hock, 1999; Olson et al., 2000; Dundr and Misteli, 2001; Ogg and Lamond, 2002; Carmo-Fonseca, 2002b]. In addition, the CBs are frequently located close to or within the nucleoli and coilin, the major protein responsible for CBs formation, has been shown to mediate communication between the two compartments [Lyon et al., 1997; Sleeman et al., 1998; Shpargel et al., 2003]. Finally, a recent extensive proteomic analysis performed on purified nucleoli revealed the complexity and the interplay between the different nuclear structures [Andersen et al., 2002].

We have previously shown, using transient transfection experiments with an ISG20 protein fused to the HA epitope peptide from influenza virus, that the ectopic ISG20 fusion protein localized in the nucleus within the promyelocytic leukemia (PML) nuclear bodies (PML-NBs) [Gongora et al., 1997]. The list of proteins associated with PML-NBs is growing [Negorev and Maul, 2001]. However, now it appears clearly that the identification of PML-NBs-associated proteins by means of transient transfection and with an artificially integrated gene locus is not a reliable method and often leads to aberrant cellular distribution [Maul et al., 2000; Tsukamoto et al., 2000; Borden, 2002]. Thus, to definitely analyze the subcellular distribution of the endogenous ISG20, in physiologically relevant experiments, specific mouse antibodies were generated against the recombinant protein [Espert et al., 2003]. In this report, using confocal immunofluorescence microscopy and electronic microscopy we show that ISG20 is clearly not associated with PML-NBs. We find that in addition to a diffuse cytoplasmic localization, ISG20 appeared concentrated in the nucleus both in the nucleolus and in the CBs. Using immunoprecipitation experiments, we show that ISG20 interacted with the survival motor neuron (SMN) protein considered to be the master assembler of macromolecular complexes involved in ribonucleoprotein and ribosome assembly. Accordingly, U1 and U2 snRNAs, and U3 snoRNA were co-immunoprecipitated with ISG20. Altogether, these data strongly suggest that ISG20 might play a role in the maturation of snRNAs and rRNAs, and in ribosome biogenesis.

MATERIALS AND METHODS

Cell Culture

Human HeLa cells were cultured at 37°C in Dulbecco's modified Eagles' medium supplemented with 10% fetal bovine serum (FBS). Human lymphoblastoid Daudi cells were cultured in RPMI 1640 supplemented with 10% FBS. For immunofluorescence assays, HeLa cells were cultured on glass slides and Daudi cells were adhered on polylysine coated glass slides just before fixation. Human α2aIFN (Intron A) was purchased from Schering-Plough.

Transient Transfections

For immunofluorescence analysis, transient transfections were carried out using the Lipofectamine Plus Reagent method according to the manufacturer's instructions (Invitrogen, France). HeLa cells were cultured on 6-well plates and transfected with 500 ng of a coilin-dsRed expression vector [Boulon et al., 2002]. Twenty-four hours after transfection, the cells were washed and fixed with 100% cold methanol for 5 min at −20°C, prior to immunofluorescence. For immunoprecipitation experiments, 4 μg of pEGFP, pEGFP-ISG20, or pEGFP-mutISG20 expression vectors [Espert et al., 2003] were transfected on 100-mm culture dishes.

Antibodies

Specific mouse and rabbit ISG20 polyclonal antibodies were previously described [Espert et al., 2003]. Rabbit PML polyclonal antibodies were purchased from Santa Cruz Biotechnologies. Rabbit anti-coilin antibodies were kindly provided by Dr. A. Lamond (Dundee, UK). The monoclonal anti-coilin and anti-SMN antibodies were purchased from BD Transduction Laboratories (BD Biosciences, France). The polyclonal rabbit fibrillarin antibody was purchased from Santa Cruz (Santa Cruz, California). Texas-Red-conjugated and fluorescein-conjugated (FITC-conjugated) secondary antibodies were purchased from Beckman Coulter (Marseille, France). Anti-GFP mouse monoclonal antibody was purchased from Roche Diagnostic (France).

Immunofluorescence Analysis

For immunofluorescence staining, the cells were washed three times in phosphate-buffered saline (PBS), fixed and permeabilized with 100% cold methanol for 5 min at −20°C. The cells were then rehydrated in PBS/0.1% Tween 20 for 15 min at room temperature and incubated for 30 min in PBS/0.1% Tween 20 supplemented with 5% FBS. Staining with anti-ISG20 (1:1,000), anti-coilin (1:100), and anti PML (1:500) antibodies were carried out for 1 h in PBS/0.1% Tween 20 supplemented with 0.1% BSA. The cells were washed three times in PBS/0.1% Tween 20 and incubated for 30 min with the secondary antibodies; Texas-Red-conjugated (1:100) or FITC-conjugated (1:1,000). Then, the nuclei were stained with DAPI (Sigma) at 2.5 μg/ml for 5 min and finally the cells were washed three times in PBS/0.1% Tween 20. For the antigen competition assay, the immunofluorescence protocol was the same as described above except that recombinant glutathione *S*-transferase (GST)-ISG20 (GST-ISG20) or GST alone, produced in the BL21-DE3 *E. coli* strain and purified by affinity chromatography on glutathione Sepharose, was added to anti-ISG20 serum before incubation with fixed HeLa cells. Imaging was performed at the CNRS-UPR 1086 CRBM Imaging Facility. For single immunostaining, images were acquired with a micromax 1300YHS CCD camera (Princeton Instruments) on a Leica DMRA microscope (Leica Microsystems) and stored as single TIFF images using METAMORPH software (Universal Imaging). For double immunostaining, A DMR B Leica confocal laser-scanning microscope equipped with an argon/krypton ion laser was used with a 100× PL APO HCX CS oil immersion objective. The microscope was fitted with a Nipkoff disk device (Perkin Elmer Ultraview). Images were captured with a coolsnap HQ (Photometrics) camera driven by Meta-Morph software (version 4.11; Universal Imaging, Westchester, PA). Images were processed using Adobe Photoshop software.

Immunoelectron Microscopy

Cells were fixed with 1.6% glutaraldehyde in Sörensen phosphate buffer at 4°C during 1 h at pH 7.3. The cells were then scraped and centrifuged at 3,000*g* for 10 min. The cell pellets were washed three times in phosphate buffer then sequentially dehydrated in methanol (30% and 50% each for 5 min at 4°C, 70% and 90%, respectively, 5 and 30 min at −20°C). This was followed by mixtures of 1:1 proportion of 90%

methanol/Lowicryl K4M (Chemische Werke Lowi, Waldkraiburg) for 1 h at −20°C, then mixture of 90% methanol/ Lowicryl K4M (1:2, v/v) for 1 h at −20°C, finally 2 volumes of pure Lowicryl K4M for 1 h at −20°C and overnight with pure Lowicryl. Cell pellets were transferred to pure Lowicryl capsules and polymerization was induced by UV irradiation for 5 days at −30°C, followed by one more day at room temperature. Ultra-thin sections on gold grids were sequentially incubated with 5% BSA in PBS for 30 s and with anti-ISG20 serum diluted 1:50 for 1 h, then with the secondary antibody (mouse anti-IgG) conjugated to 10 nm gold particles (Biocell Research Laboratories, Cardiff) diluted 1:30 in PBS (30 min). Finally, the sections were washed and stained with 5% aqueous uranyl acetate before their observation with a ZEISS 902 electron microscope at 80 kV.

Immunoprecipitation and Protein Analysis

The cells were resuspended in PBS lysis buffer containing: 0.5% Triton X-100, 1 mM DTT, 100 μM phenylmethylsulphonyl fluoride (PMSF), protease inhibitor cocktail (1 tablet/10 ml, Roche Diagnostics), and 0.1 U/μl RNase inhibitor RNasin (Promega). Supernatant (10,000*g*) was prepared and used for immunoprecipitation. Extracts were incubated for 1 h at 4°C with either anti-ISG20 or anti-GFP antibodies. The extracts were then mixed with 30 μl of sheep anti-mouse IgG attached to magnetic beads (Dynabeads, Dynal France) and incubated for 1 h at 4°C. The beads were washed five times in PBS lysis buffer. The immunoprecipitated proteins were resuspended in 20 μl of loading buffer (10 mM Tris-HCl pH 6.8, 1% SDS, 5 mM EDTA, and 50% glycerol), incubated for 5 min at 95°C, fractionated on a 12% SDS–PAGE, and transferred onto PVDF membrane. After a blocking step, the membrane was incubated with the appropriate antibody and then developed using a chemiluminescent detection system (ECL-Plus, Amersham Pharmacia Biotech).

To obtain cytoplasmic and nuclear extracts, the cells were resuspended in 10 volumes of PBS buffer diluted 1:4 and containing: 0.5% Triton X-100, 1 mM DTT, 100 μM PMSF, protease inhibitor cocktail, and 0.1 U/μl RNase inhibitor RNasin. Cytoplasmic extracts were separated from nuclei by centrifugation at 1,260*g*, cleared by an additional centrifugation at 10,000*g* for 10 min and then adjusted to 200 mM NaCl. The nuclei pellets were resuspended in PBS lysis buffer adjusted to 200 mM NaCl. After 15 min incubation, the nuclear extracts were recovered by centrifugation at 12,000*g* for 10 min. For immunoprecipitations, highly affinity purified rabbit polyclonal anti-ISG20 antibodies were covalently linked to tosyl-activated magnetic beads as described by the manufacturer (Dynal, France).

Northern Blot Analysis

Immunoprecipitates were resuspended in formamide loading buffer and fractionated through a 6% polyacrylamide-7M urea gel, transferred onto a nylon membrane (Hybond N^+, Amersham Pharmacia) and hybridized to 10^7 cpm/ml of [32P]-labeled U1, U2, or U3 cDNA probe. Membranes were washed to a final stringency of 0.2× SSC/0.1% SDS (1× SSC is 0.15M sodium chloride and 0.015M sodium citrate, pH 7.0), at 42°C before autoradiography.

RESULTS

Subcellular Distribution of ISG20 Protein

To analyze the subcellular distribution of the endogenous ISG20, specific mouse antibodies were generated against a glutathione *S*-transferase (GST)-ISG20 (GST-ISG20) fusion protein and their specificity established by Western blot [Espert et al., 2003]. Antiserum stainings were performed on HeLa cells using microscopic immunofluorescence. In addition to a diffuse cytoplasmic and nucleoplasmic localization, ISG20 also appeared to be concentrated in the nucleus both in the nucleoli and in two to three bright discrete punctuated intranuclear structures (Fig. 1A). As negative control, immunofluorescence analysis was performed with the antiserum anti-ISG20 or with the FITC-conjugated mouse secondary antibody used alone (data not shown). The same staining pattern was observed from anti-ISG20 antiserum obtained from three independently immunized mice. The specificity of the staining observed was validated by performing an antigen competition assay with GST or GST-ISG20 recombinant protein as competitor for antibody binding (Fig. 1B,C). The recombinant GST-ISG20 protein fully reversed the staining, whereas in competition experiments performed with GST control protein, no reduction in the staining was observed. These data demonstrated the ability

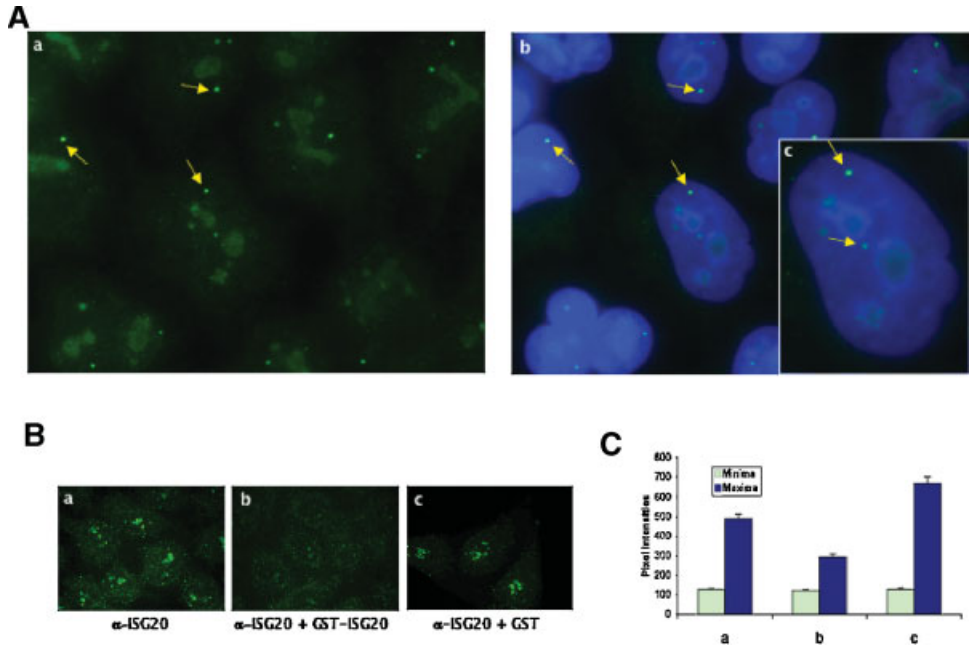

Fig. 1. Subcellular localization of ISG20. **A**: HeLa cells were fixed for 5 min at −20°C in 100% methanol. **a**: The cells were labeled with mouse polyclonal anti-ISG20 antibodies and revealed with a FITC-conjugated secondary antibody. **b**: Overlay of nuclear DAPI staining and ISG20 staining. **c**: High magnification of a labeled nucleus is presented. The yellow arrows indicate specific dots in the cell nucleus. **B**: Recombinant ISG20 selectively competes with ISG20 antibody labeling. HeLa cells were labeled using mouse anti-ISG20 antibodies in absence (a) or presence of either GST-ISG20 (b), or GST alone (c) recombinant protein at 200 μg/ml, and then revealed by a FITC-conjugated secondary antibody. **C**: Pixel intensities of ISG20 labeling presented in (B), performed in absence (a) or in presence of either GST-ISG20 (b) or GST alone (c) were recorded using Metamorph software (Universal Imaging corp.). Minima (background level) and maxima (ISG20 specific staining signal) intensities were recorded using constant nuclear areas. The measurements from 16 different cells of each labeling experiment (a, b, and c) were averaged and plotted ± SD.

of our mouse serum anti-ISG20 to detect endogenous ISG20 protein.

ISG20 Accumulates in Cajal (Coiled) Bodies Nuclear Structures

In addition to the nucleoli staining, the antiserum anti-ISG20 typically labeled two to three punctuated structures scattered in the nucleoplasm around the nucleoli (Fig. 1). This punctuated nuclear pattern is reminiscent of the labeling observed for the CBs. [Bellini, 2000; Gall, 2000; Lam et al., 2002]. Indeed, several observations are consistent with this analysis. First, the nucleoli and the CBs are physically and functionally closely associated [Gall, 2001; Ogg and Lamond, 2002; Carmo-Fonseca, 2002b], and the CBs were first described as "nucleolar accessory bodies" by their discoverers [Cajal, 1903]. Second, the CBs are highly mobile structures and have the ability to move to and from the nucleolar periphery and within the nucleolus [Platani et al., 2000]. Finally, using snRNP proteins in fusion with the green fluorescent protein (GFP), dynamic interactions between components of the CBs and the nucleoli have been demonstrated [Sleeman et al., 1998]. We have previously shown that, in transient transfection experiments with an ISG20 protein fused to the HA epitope from influenza virus, the ectopic ISG20 protein localized in the nucleus within the promyelocytic leukemia nuclear bodies (PML-NBs) [Gongora et al., 1997]. To clarify this discrepancy, double staining immunofluorescence experiments were performed in physiologically relevant experiments on HeLa cells with anti-ISG20 antibodies and either antibodies against the CBs signature protein, p80-coilin [Andrade et al., 1991], or anti-PML polyclonal antibodies. The confocal fluorescence micrographs presented in Figure 2A-a and -b, show that, except for the nucleolar labeling, the nuclear pattern of endogenous ISG20 and p80-coilin immunostaining are similar. The superimposition of the single confocal images reveals that the two proteins perfectly colocalize in the small-punctuated structures (Fig. 2A-c). In contrast, the pattern observed for PML immunostaining presented

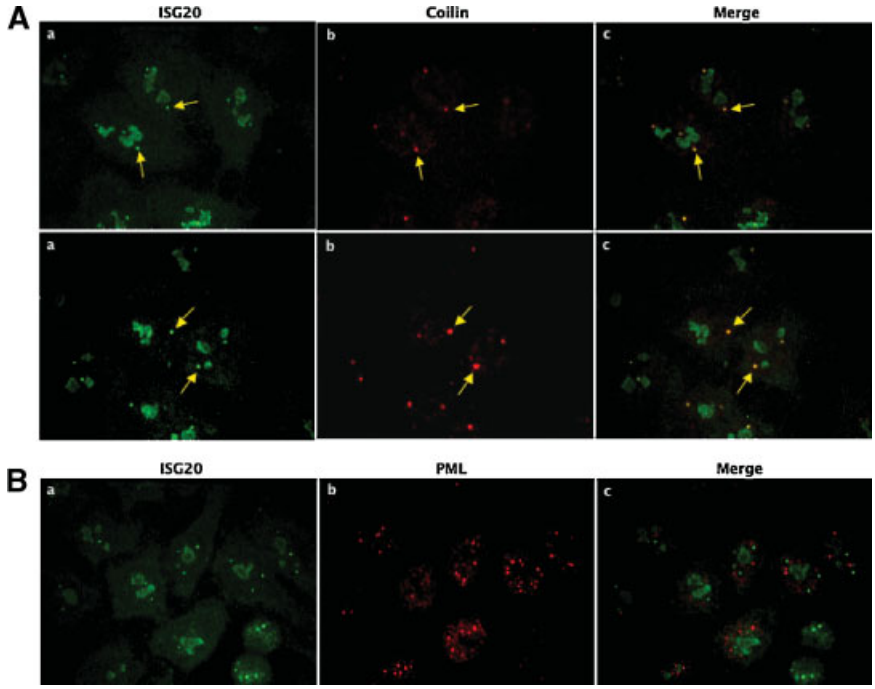

Fig. 2. ISG20 colocalizes with the coilin protein in CBs. **A**: Double-labeling of HeLa cells was performed using mouse anti-ISG20 antibodies and specific rabbit polyclonal anti-coilin antibodies. ISG20 was revealed with a FITC-conjugated secondary antibody (**a**) and Coilin with a Texas-Red-conjugated secondary antibody (**b**). The overlay of the two images is presented (**c**). The arrows in each image indicate the labeled CBs. **B**: Double-labeling of HeLa cells was performed using mouse anti-ISG20 antibodies and specific rabbit polyclonal anti-PML antibodies. ISG20 is revealed with a FITC-conjugated secondary antibody (a) and PML with a rabbit Texas-Red-conjugated secondary antibody (b). Superimposed images are shown (c).

many more punctuated structures that are clearly not coincident with ISG20 labeling (Fig. 2B). It should be noted that the pattern of ISG20 labeling is similar in the presence of PML and in the PML−/− cells (data not shown). As the absence of PML results in a diffuse distribution of all other NBs-associated proteins, these data clearly confirmed that ISG20 is not NBs-associated.

To strengthen our finding, we analyzed the colocalization between endogenous ISG20 and an ectopically expressed coilin-red fluorescent fusion protein (coilin-dsRed) [Boulon et al., 2002]. HeLa cells were transfected with the coilin-dsRed-expressing construct, as described in Materials and Methods. Twenty-four hours later, transfected cells were detected by red fluorescence, and ISG20 protein expression was monitored by immunofluorescence using the mouse polyclonal anti-ISG20 antibody. The ectopically expressed coilin-dsRed presented a punctuated pattern with numerous nuclear dots (Fig. 3b). These data are not surprising because coilin is responsible for regulating the number of CBs [Ogg and Lamond, 2002]. In particular, it has been previously shown that ectopic expression of a coilin fusion protein with the GFP at its C-terminus led to a striking

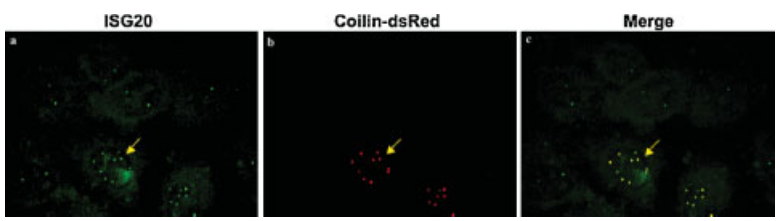

Fig. 3. Endogenous ISG20 colocalizes with ectopically expressed coilin. The coilin-dsRed expression vector (0.5 μg) was transfected in HeLa cells using the Lipofectamine Plus Reagent protocol. Twenty-hours later, cells were single-labeled with the anti-ISG20 antibodies and revealed with a FITC-conjugated secondary antibody (**a**). Coilin-dsRed is visualized in red (**b**) and the two images were superimposed (**c**).

increase in the number of CBs [Shpargel et al., 2003]. Concomitantly with a higher number of CBs, the number of nuclear dots containing ISG20 also increases (Fig. 3a). Moreover, the two proteins perfectly colocalized in these structures (Fig. 3c). Taken together, all these experiments demonstrated that, beside its presence in the nucleolus, ISG20 is associated with the CBs.

IFN Treatments of HeLa or Daudi Cells Increase ISG20 Expression in the CBs

CBs and the nucleoli are typically highly dynamic nuclear structures. In particular, various stimuli such as viral infections [Matthews, 2001; Hiscox, 2002] or specific inhibition of rRNA transcription [Schofer et al., 1996; Chen and von Mikecz, 2000] can cause the redistribution of nucleolar-associated proteins. Interestingly, it has been suggested that the inhibition of cell proliferation by IFN might partly result from the inhibition of rRNA transcription mediated by the IFN-induced p202 protein [Liu et al., 1999]. As ISG20 is an IFN-inducible protein [Gongora et al., 1997; Gongora et al., 2000], we addressed the question of whether treatment of HeLa and lymphoblastoid Daudi cells with IFN could alter its cellular distribution. To this end, both HeLa and Daudi cells were cultured for 16 h in absence or presence of 500 U/ml of human α2aIFN (Hu-α2aIFN). Single immunofluorescence stainings were performed with either anti-ISG20 antibodies or anti-coilin antibodies, as previously described. No apparent cellular redistribution of ISG20 and coilin proteins were observed

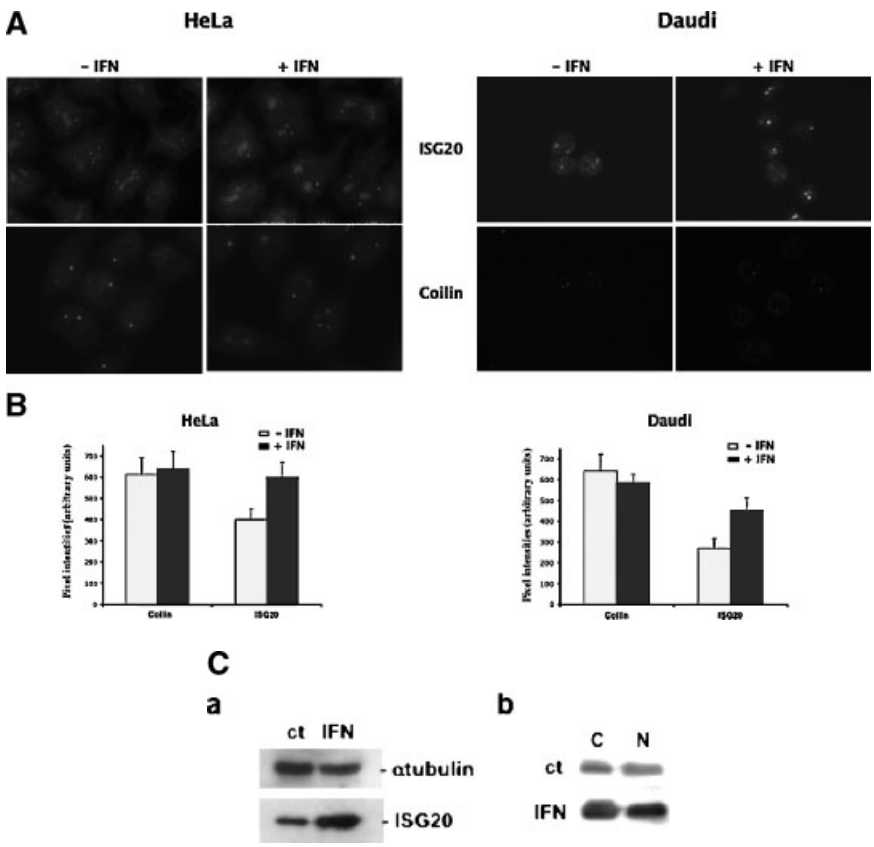

Fig. 4. IFN treatments of HeLa or Daudi cells increase ISG20 expression in the Cajal bodies. **A**: HeLa and Daudi cells untreated (*−IFN*) or treated (*+IFN*) for 16 h with 500 U/ml of Hu-α2aIFN were fixed for 5 min at −20°C in 100% methanol. Subsequently, cells were labeled with either mouse polyclonal anti-ISG20 antibodies or with mouse monoclonal anti-coilin antibodies and revealed with the FITC-conjugated secondary antibody for ISG20 or TRITC-conjugated secondary antibody for Coilin. **B**: For each experimental condition, pixel intensities of individual spots were recorded using Metamorph software (Universal Imaging corp.). The histograms represent the mean of intensities measured for at least 20–30 ISG20 or coilin dot spots in absence (*fill white*) or presence (*fill black*) of IFN. **C**: (**a**) Whole protein extracts from Daudi cells untreated (*ct*) or treated for 16 h with 500 U/ml of α2aIFN were prepared and analyzed by immunoblotting with specific rabbit anti-ISG20 antibodies. Expression of αtubulin was used as an invariant control. (**b**) Cytoplasmic and nuclear extracts were prepared from Daudi cells and analyzed by immunoblotting with rabbit anti-ISG20 antibodies.

following Hu-α2aIFN treatment (Fig. 4A). However, ISG20 staining appeared significantly increased both in the cytoplasm and in the CBs. No significant variation of ISG20 nucleoli staining was observed. In addition, pixel intensity analysis of at least 20–30 ISG20 or coilin individual spots confirmed that ISG20 was significantly upregulated by IFN, whereas coilin remained invariant in the CBs (Fig. 4B). To confirm these data, the ISG20 subcellular distribution was carried out by Western blotting analysis of subcellular fractions prepared from HeLa cells, as described in Materials and Methods. As expected, ISG20 protein is present in both the cytoplasmic and the nuclear fraction and the protein is induced by Hu-α2aIFN in these two compartments (Fig. 4C).

ISG20 Protein Concentrates in the Dense Fibrillar Component (DFC) of the Nucleolus

The overlay of ISG20 and the morphological nucleolar marker fibrillarin immunostaining images confirmed that ISG20 was also localized in the nucleoli (Fig. 5A-c). The nucleolus can be subdivided in three morphologically and functionally distinct subcompartments; the fibrillar center (FC), the dense fibrillar component (DFC), and the granular component (GC). It is usually admitted that the early steps of rRNA processing occur in the DFC, whereas the later steps and ribosome assembly occur in the GC [Scheer and Hock, 1999; Dundr and Misteli, 2001; Carmo-Fonseca, 2002b]. These three components reflect the vectorial process of ribosome biogenesis [Dundr and Misteli, 2001]. We used immunoelectron microscopy to accurately determine the nucleolar localization of ISG20. The electron micrographs presented in Figure 5B show that gold particles are mainly located over the DFC on HeLa cells (Fig. 5B-a). Very few gold particles are present over the GC, whereas the FC component is unlabeled. The reorganization of nucleolar ultrastructures by actinomycin D has been described associated with the inhibition of rRNA synthesis [Puvion-Dutilleul et al., 1992]. In particular, this treatment leads to the segregation of the three components of the nucleolus, allowing the visualization of each of them independently [Puvion-Dutilleul et al., 1992]. Accordingly, in actinomycin D-treated HeLa cells (Fig. 5B-b), gold particles are principally concentrated in the DFC. Altogether, these experiments demonstrate that the exonuclease ISG20 protein

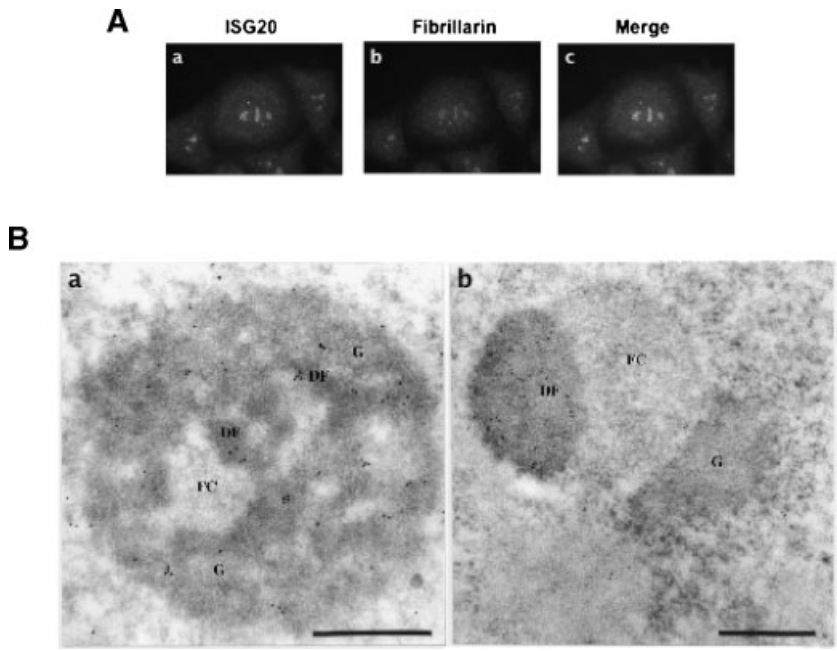

Fig. 5. ISG20 localizes within the dense fibrillar component of the nucleolus. **A**: HeLa cells were labeled with mouse polyclonal anti-ISG20 antibodies and with specific rabbit polyclonal anti-fibrillarin antibodies. ISG20 was revealed with a FITC-conjugated secondary antibody (**a**) and fibrillarin with a Texas-Red-conjugated secondary antibody (**b**). The superimposition of the two pictures is represented (**c**). **B**: ISG20 was revealed by electron microscopy in the nucleolus of untreated (a) or actinomycin D treated (b) HeLa cells. Granular (G), fibrillar center (FC) and dense fibrillar (DF) components are indicated. Scale bar, 0.5 μm.

mainly localized in the DFC, the major site described for rRNA processing in the nucleolus [Puvion-Dutilleul et al., 1992; Andersen et al., 2002; Carmo-Fonseca, 2002a], suggesting that ISG20 might be involved in the processing of rRNA.

ISG20 Was Associated With Nuclear SMN-Containing Macromolecular Complexes

SMN is part of a large complex of proteins required for the biogenesis of various snRNPs [Fischer et al., 1997; Liu et al., 1997]. The protein mainly localizes in both the cytoplasm and in the CBs [Liu and Dreyfuss, 1996]. In particular, CBs appear to be the nuclear sites where SMN facilitates assembly of various diverse cellular complexes [Terns and Terns, 2001]. However, SMN was also found in the nucleoli of neuronal cells [Lefebvre et al., 2002; Wehner et al., 2002] and in fetal tissues [Young et al., 2001]. In addition, coilin was shown to be the factor responsible for targeting SMN to CBs [Hebert et al., 2001; Tucker et al., 2001; Hebert et al., 2002]. The exonuclease activity of ISG20 and its subcellular distribution led us to imagine that ISG20 could interact with the SMN macromolecular complex. To evaluate this hypothesis, whole protein extracts from HeLa cells were prepared and subjected to immunoprecipitations with highly affinity purified rabbit polyclonal anti-ISG20 antibodies covalently linked to tosyl-activated magnetic beads. The immunoprecipitates were then analyzed by Western blotting using a specific anti-SMN monoclonal antibody. The results presented in Figure 6A show that SMN was efficiently co-precipitated with ISG20 (lane 3). No co-precipitation was detectable in experiments performed in absence of anti-ISG20 antibodies (lane 4). To strengthen our finding, HeLa cells

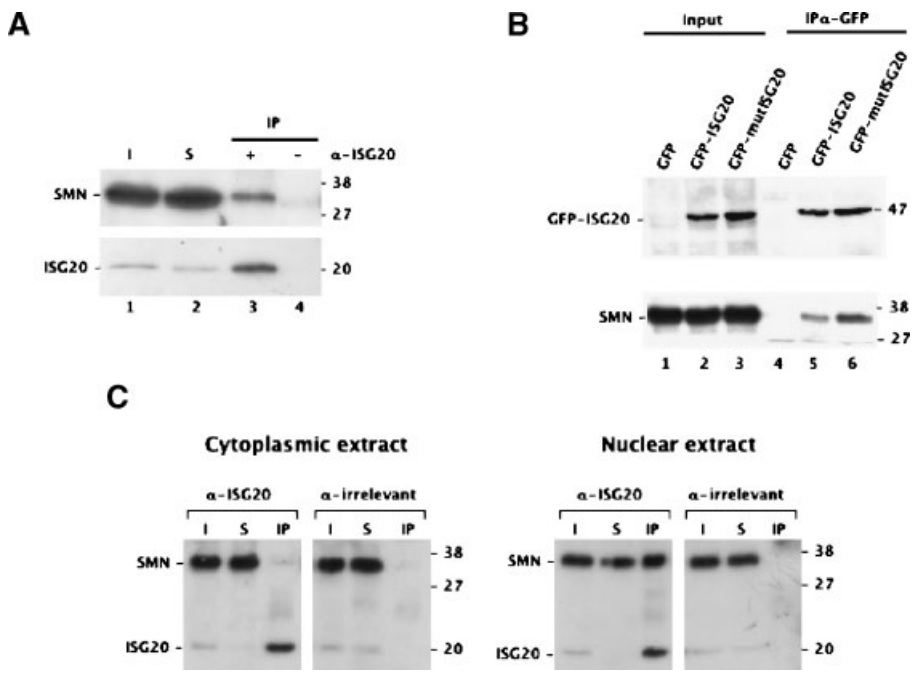

Fig. 6. ISG20 belongs to a nuclear-SMN containing complex. **A**: Total protein extracts from HeLa cells were subjected to immunoprecipitation with the anti-ISG20 antibody covalently linked to tosyl-activated magnetic beads as described in Materials and Methods. Immunoprecipitated proteins were then fractionated by SDS–PAGE and revealed by Western blotting with either anti-SMN or anti-ISG20 antibodies. The inputs (lane 1) and the supernatants after immunoprecipitation (lane 2) show 4% of the lysate used in the immunoprecipitation reactions. As control, the immunoprecipitation was performed in absence of anti-ISG20 antibodies (lane 4). **B**: HeLa cells were transfected with the pEGFP vector or with vectors expressing either a GFP-ISG20 fusion protein or the GFP protein fused with an inactive mutated ISG20 protein (GFP-mutISG20). Whole protein extracts were prepared and subjected to immunoprecipitations with a mouse polyclonal anti-GFP antibody. The immunoprecipitates were then analyzed by Western blotting using the anti-ISG20 (*top*) or anti-SMN antibodies (*bottom*). **C**: Cytoplasmic and nuclear extracts were prepared from Daudi cells and subjected to immunoprecipitations with highly affinity purified rabbit polyclonal anti-ISG20 antibodies and irrelevant rabbit polyclonal antibodies covalently linked to tosyl-activated magnetic beads as described in Materials and Methods. The immunoprecipitates were then analyzed by Western blotting using the anti-ISG20 or anti-SMN antibodies. The lanes corresponding to the input (I), the supernatants after immunoprecipitation (S), and the immunoprecipitates (IP) are indicated.

were transfected with vectors expressing either a GFP-ISG20 fusion protein or the GFP-fused with an inactive mutated ISG20 protein (GFP-mutISG20) [Espert et al., 2003]. The empty pEGFP vector, expressing GFP protein alone was used as a negative control. Twenty-four hours after transfection, whole protein extracts were prepared and subjected to immunoprecipitations with a mouse monoclonal anti-GFP antibody. The immunoprecipitates were then analyzed by Western blotting using the anti-SMN or anti-ISG20 antibody. As expected, the results presented on Figure 6B show that SMN was immunoprecipitated by the anti-GFP antibody from cellular extract of GFP-ISG20 transfected cells (lane 5). No immunoprecipitation was detected from cells transfected with the empty pEGFP vector (lane 4). In accordance with the previously described dominant-negative activity of mutISG20, SMN also associated with GFP-mutISG20 protein (lane 6).

Like ISG20, SMN is present in both the cytoplasm and in the CBs. So, we next investigated the cellular distribution of ISG20/SMN-containing complexes. Cytoplasmic and nuclear extracts were prepared from Daudi cells, as described in Materials and Methods, and subjected to immunoprecipitations with anti-ISG20 antibodies covalently linked to tosyl-activated magnetic beads. The immunoprecipitates were analyzed by Western blotting using the anti-SMN or anti-ISG20 antibody. Interestingly, SMN was co-immunoprecipitated with ISG20 from nuclear extracts (Fig. 6C). No co-precipitation was detectable from cytoplasmic extracts suggesting that ISG20/SMN-containing complexes were only present in the CBs. Neither SMN nor ISG20 was immunoprecipitated with an irrelevant rabbit polyclonal antibody demonstrating the specificity of the immunoprecipitation. Similar data were obtained with extracts prepared from HeLa cells (data not shown). These data clearly demonstrate that ISG20 was associated with SMN-containing macromolecular nuclear complexes.

Small Nuclear RNAs Co-Immunoprecipates With ISG20

SMN macromolecular complexes are characterized by ultrastructured RNA-proteins interactions. In particular, SMN is considered to be the master assembler of snRNPs and snoRNPs ribonucleoproteic complexes. To assay the capability of ISG20 to associate with complexes containing snRNPs or snoRNPs, HeLa cells were transfected with pEGFP, pEGFP-ISG20, or pEGFP-mutISG20 expression vectors, as previously described. Cell lysates were prepared and subjected to immunoprecipitation using monoclonal anti-GFP antibodies. The immunoprecipitates were resuspended in formamide loading buffer and resolved on a 6% polyacrylamide-7M urea gel. After electrotransfert to a nylon support, the blot was analyzed for the presence of U1, U2, and U3 RNA. As shown in Figure 7, U1, U2, and U3 RNAs were co-immunoprecipitated with GFP-ISG20 and GFP-mutISG20 proteins. No RNAs were detected when immunoprecipitation experiments were performed from cells transfected with the empty pEGFP vector. These data demonstrate that ISG20 is a component of ribonucleoproteic complexes.

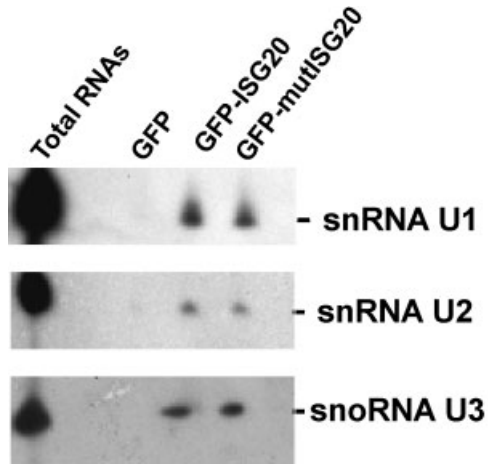

Fig. 7. Small nuclear RNAs co-immunoprecipitate with ISG20. HeLa cells were transfected with the pEGFP vector or with vectors expressing either GFP-ISG20 or GFP-mutISG20 fusion proteins. Whole protein extracts were prepared and subjected to immunoprecipitations with a mouse polyclonal anti-GFP antibody. RNAs present in the immunoprecipitates were analyzed by Northern blot for the presence of U1 and U2 snRNAs, and U3 snoRNA. As positive control, total cellular RNAs were loaded onto the gel.

DISCUSSION

In this report, using confocal immunofluorescence and electron microscopy analysis, we show that ISG20, a 3′ to 5′ exoribonuclease, is a component of both the CBs and the DFC region of the nucleolus. It is well established that the nucleolus is the site of rRNA maturation and ribosome biogenesis [Dundr and Misteli, 2001].

In particular, DFC is described as the major site for the late step of rRNA maturation [Puvion-Dutilleul et al., 1992; Andersen et al., 2002; Carmo-Fonseca, 2002a]. The fact that ISG20 is a 3′ to 5′ exoribonuclease and appears principally concentrated in the DFC, strongly suggests that it might be involved in the maturation of rRNA and ribosome biogenesis. These processes are highly conserved during evolution. In eukaryotes, they are best characterized in the yeast *Saccharomyces cerevisiae* [Raue and Planta, 1991; Cockell and Gasser, 1999; Kressler et al., 1999]. Notably, the Rrp5p protein is known to be required for the processing of pre-rRNA, particularly in the formation of both 18S and 5.8S rRNA [Venema and Tollervey, 1996]. A recent study shows that particular motifs of Rrp5p are crucial for the correct assembly and action of the processing complex responsible for maturation of rRNA [Eppens et al., 2002]. More importantly, a synthetic lethality screen using a Rrp5p mutant resulted in the isolation of the *REX4* gene, encoding the protein Rex4p, belonging to the DEDD family of $3' \rightarrow 5'$ exonucleases. The authors clearly implicate the *REX4* gene in the pre-rRNA processing in yeast Rrp5p mutants [Eppens et al., 2002]. Interestingly, ISG20 is a human homolog of the Rex4p. These data and the nucleolar localization of ISG20 strongly strengthen our hypothesis on the role of ISG20 in the maturation of rRNA in humans.

The actual implication of ISG20 in the CBs appears more complicated. First described as accessory bodies of the nucleolus [Cajal, 1903], the CBs now appear as a traffic area necessary for the maturation of snoRNAs before their nucleolar translocation. In particular, the U3 snoRNA synthesized in the nucleoplasm is 3′-end processed by an unknown exonuclease within the CBs before association with the common snoRNA binding protein, fibrillarin [Herrera-Esparza et al., 2002; Verheggen et al., 2002]. Then, the mature U3 snoRNPs are imported to the nucleoli where they act as guide RNAs in pre-rRNA cleavage during ribosome biogenesis [Gerbi and Borovjagin, 1997; Scheer and Hock, 1999; Dragon et al., 2002; Verheggen et al., 2002; Carmo-Fonseca, 2002b]. On the basis of these observations, it is tempting to speculate that ISG20 can participate in the maturation of U3 snoRNA and then be transported in the DFC with the large ribonucleoprotein U3 to participate in the final steps of rRNA processing. However, the CBs were also suspected to be the cellular sites for post-transcriptional modifications and final maturations of spliceosomal snRNAs U1, U2, U4, and U5 prior to their migration in the splicing speckles bodies, another distinct nuclear structure [Sleeman et al., 2001; Darzacq et al., 2002; Jady et al., 2003]. Thus, we cannot exclude that ISG20 might be more generally involved in the maturation of several RNA species. In accordance with this hypothesis, we demonstrated that U1 and U2 snRNAs, and U3 snoRNA were co-immunoprecipitated with ISG20. Finally, the nucleolus and CBs are highly mobile structures, and dynamic interplays occur between the two compartments [Dundr and Misteli, 2001; Ogg and Lamond, 2002; Carmo-Fonseca, 2002c]. CBs are frequently located close to or within the nucleoli, and numerous proteins, like the RNase P and MRP subunits Rpp29 and Rpp38 [Jarrous et al., 1999], fibrillarin and Nopp140 [Jarrous et al., 1999; Dundr and Misteli, 2001] are present in both compartments [Lyon et al., 1997; Sleeman et al., 1998; Shpargel et al., 2003]. Altogether, these reports and our own observations strongly implicate ISG20 in events of RNA maturation involving exchange processes between the CBs and the nucleoli.

We also present evidences that ISG20 is associated with nuclear SMN-containing macromolecular complexes. SMN protein is part of a large complex that is required for biogenesis of various snRNPs [Fischer et al., 1997; Liu et al., 1997; Meister et al., 2000; Pellizzoni et al., 2001; Terns and Terns, 2001]. Recently, it has been shown that SMN interacts directly with the coilin and that this interaction mediates recruitment of both SMN complex and splicing snRNPs to the CBs [Hebert et al., 2001]. Moreover, SMN is suggested to be responsible for the assembly of CBs [Gall, 2000; Jones et al., 2001; Massenet et al., 2002]. Furthermore, like ISG20, SMN localizes both in the cytoplasm and in the CBs [Liu and Dreyfuss, 1996; Matera and Frey, 1998; Carvalho et al., 1999]. Indeed, SMN is involved in the cytoplasmic maturation of snRNPs, with a possible role in the reimport process [Massenet et al., 2002; Narayanan et al., 2002]. Thus, it is probable that SMN is associated with snRNPs along their biogenesis and leads them to the CBs where their maturation is achieved. It is for this reason that CBs have been suggested to play a role in the later stages of snRNP modification and assembly [Sleeman

et al., 2003]. However, the fact that ISG20/SMN-containing complexes seem to be mainly localized in the CBs, suggests that ISG20 might be involved in later stages of snRNP maturation.

The IFNs are a family of multifunctional secreted proteins characterized by their abilities to interfere with virus infection and replication [Lengyel, 1993; Player and Torrence, 1998]. They prevent viral propagation mainly by interfering with the synthesis of cellular protein [Player and Torrence, 1998]. Until now, two IFN-regulated pathways have been considered to be involved in these processes: the double-stranded RNA-dependent protein kinase R (PKR) [Meurs et al., 1990; Gale and Katze, 1998] and the 2-5A/RNase L system [Zhou et al., 1993]. PKR is a serine/threonine kinase which, after binding to dsRNA, phosphorylates the protein synthesis initiation factor eIF2 and the inhibitor of NFκB (I-κB) resulting in the inhibition of protein synthesis and in specific transcription regulation [Williams, 2001]. RNase L is a dormant cytosolic endoribonuclease that is activated by short oligoadenylates produced by the 2′-5′ oligoadenylate synthetase (2-5OAS) following viral infection or IFN exposure [Stark et al., 1998]. Degradation of viral RNAs and cleavage of cellular 18S and 28S rRNAs by activated-RNAse L lead to the inhibition of protein synthesis [Player and Torrence, 1998]. The potential involvement of ISG20 in snRNA, snoRNA, and rRNA metabolism implies the possibility of a new pathway participating in the antiviral effects of IFNs. The noticeable IFN-induced accumulation of ISG20 in the CBs, where the exonuclease can interfere with snRNPs, snoRNPs, and rRNAs formation, strongly suggests the involvement of ISG20 in a new route for IFN-mediated control of protein synthesis, namely by modulating both snRNAs and rRNAs maturation. Obviously, further studies are needed to determine exactly the biological contribution of ISG20 in these processes. Unfortunately, attempts to inhibit ISG20 expression by small interfering RNAs (siRNA) have remained unsuccessful because ISG20 expression is strongly and non-specifically induced by siRNA. The elucidation of the exact functions of this highly regulated 3′ to 5′ exonuclease, will probably emerge from proteomic approaches aimed at the identification of direct molecular partners of ISG20.

ACKNOWLEDGMENTS

We thank Dr. A. Lamond for providing the anti-coilin antibodies, Evelyne Pichard for technical assistance in electron microscopy experiments, and Pierre Travo for technical assistance for confocal immunofluorescence analysis. We also thank Dr. S. L. Salhi for presubmission editorial assistance. Lucile Espert was supported by fellowships from the Association pour la Recherche contre le Cancer and Sidaction-Ensemble Contre le Sida.

REFERENCES

Andersen JS, Lyon CE, Fox AH, Leung AK, Lam YW, Steen H, Mann M, Lamond AI. 2002. Directed proteomic analysis of the human nucleolus. Curr Biol 12:1–11.

Andrade LE, Chan EK, Raska I, Peebles CL, Roos G, Tan EM. 1991. Human autoantibody to a novel protein of the nuclear coiled body: Immunological characterization and cDNA cloning of p80-coilin. J Exp Med 173:1407–1419.

Beelman CA, Parker R. 1995. Degradation of mRNA in eukaryotes. Cell 81:179–183.

Bellini M. 2000. Coilin, more than a molecular marker of the cajal (coiled) body. Bioessays 22:861–867.

Borden KL. 2002. Pondering the promyelocytic leukemia protein (PML) puzzle: Possible functions for PML nuclear bodies. Mol Cell Biol 22:5259–5269.

Boulon S, Basyuk E, Blanchard JM, Bertrand E, Verheggen C. 2002. Intra-nuclear RNA trafficking: Insights from live cell imaging. Biochimie 84:805–813.

Cajal SR. 1903. Un sencillo método de coloracion selectiva del reticulo protoplasmico y sus efectos in los diversos organos nerviosos de vertebrados e invertebrados. Tra Lab Invest Biol 2:129–221.

Carmo-Fonseca M. 2002a. The contribution of nuclear compartmentalization to gene regulation. Cell 108: 513–521.

Carmo-Fonseca M. 2002b. New clues to the function of the Cajal body. EMBO Rep 3:726–727.

Carmo-Fonseca M. 2002c. Understanding nuclear order. Trends Biochem Sci 27:332–334.

Carvalho T, Almeida F, Calapez A, Lafarga M, Berciano MT, Carmo-Fonseca M. 1999. The spinal muscular atrophy disease gene product, SMN: A link between snRNP biogenesis and the Cajal (coiled) body. J Cell Biol 147:715–728.

Chen M, von Mikecz A. 2000. Specific inhibition of rRNA transcription and dynamic relocation of fibrillarin induced by mercury. Exp Cell Res 259:225–238.

Cockell MM, Gasser SM. 1999. The nucleolus: Nucleolar space for RENT. Curr Biol 9:R575–R576.

Darzacq X, Jady BE, Verheggen C, Kiss AM, Bertrand E, Kiss T. 2002. Cajal body-specific small nuclear RNAs: A novel class of 2′-O-methylation and pseudouridylation guide RNAs. Embo J 21:2746–2756.

Deutscher MP, Li Z. 2001. Exoribonucleases and their multiple roles in RNA metabolism. Prog Nucleic Acid Res Mol Biol 66:67–105.

Dragon F, Gallagher JE, Compagnone-Post PA, Mitchell BM, Porwancher KA, Wehner KA, Wormsley S, Settlage RE, Shabanowitz J, Osheim Y, Beyer AL, Hunt DF, Baserga SJ. 2002. A large nucleolar U3 ribonucleoprotein required for 18S ribosomal RNA biogenesis. Nature 417:967–970.

Dundr M, Misteli T. 2001. Functional architecture in the cell nucleus. Biochem J 356:297–310.

Dundr M, Misteli T. 2002. Nucleolomics: An inventory of the nucleolus. Mol Cell 9:5–7.

Eppens NA, Faber AW, Rondaij M, Jahangir RS, van Hemert S, Vos JC, Venema J, Raue HA. 2002. Deletions in the S1 domain of Rrp5p cause processing at a novel site in ITS1 of yeast pre-rRNA that depends on Rex4p. Nucleic Acids Res 30:4222–4231.

Espert L, Degols G, Gongora C, Blondel D, Williams BR, Silverman RH, Mechti N. 2003. ISG20, a new interferon-induced RNase specific for single-stranded RNA, defines an alternative antiviral pathway against RNA genomic viruses. J Biol Chem 278:16151–16158.

Fischer U, Liu Q, Dreyfuss G. 1997. The SMN-SIP1 complex has an essential role in spliceosomal snRNP biogenesis. Cell 90:1023–1029.

Gale M, Jr., Katze MG. 1998. Molecular mechanisms of interferon resistance mediated by viral- directed inhibition of PKR, the interferon-induced protein kinase. Pharmacol Ther 78:29–46.

Gall JG. 2000. Cajal bodies: The first 100 years. Annu Rev Cell Dev Biol 16:273–300.

Gall JG. 2001. A role for Cajal bodies in assembly of the nuclear transcription machinery. FEBS Lett 498:164–167.

Gall JG, Bellini M, Wu Z, Murphy C. 1999. Assembly of the nuclear transcription and processing machinery: Cajal bodies (coiled bodies) and transcriptosomes. Mol Biol Cell 10:4385–4402.

Gerbi SA, Borovjagin A. 1997. U3 snoRNA may recycle through different compartments of the nucleolus. Chromosoma 105:401–406.

Gongora C, David G, Pintard L, Tissot C, Hua TD, Dejean A, Mechti N. 1997. Molecular cloning of a new interferon-induced PML nuclear body-associated protein. J Biol Chem 272:19457–19463.

Gongora C, Degols G, Espert L, Hua TD, Mechti N. 2000. A unique ISRE, in the TATA-less human Isg20 promoter, confers IRF-1-mediated responsiveness to both interferon type I and type II. Nucleic Acids Res 28:2333–2341.

Hebert MD, Szymczyk PW, Shpargel KB, Matera AG. 2001. Coilin forms the bridge between Cajal bodies and SMN, the spinal muscular atrophy protein. Genes Dev 15:2720–2729.

Hebert MD, Shpargel KB, Ospina JK, Tucker KE, Matera AG. 2002. Coilin methylation regulates nuclear body formation. Dev Cell 3:329–337.

Herrera-Esparza R, Kruse L, Von Essen M, Campos L, Barbosa O, Bollain JJ, Badillo I, Avalos-Diaz E. 2002. U3 snoRNP associates with fibrillarin a component of the scleroderma clumpy nucleolar domain. Arch Dermatol Res 294:310–317.

Hiscox JA. 2002. The nucleolus–a gateway to viral infection? Arch Virol 147:1077–1089.

Jady BE, Darzacq X, Tucker KE, Matera AG, Bertrand E, Kiss T. 2003. Modification of Sm small nuclear RNAs occurs in the nucleoplasmic Cajal body following import from the cytoplasm. Embo J 22:1878–1888.

Jarrous N, Wolenski JS, Wesolowski D, Lee C, Altman S. 1999. Localization in the nucleolus and coiled bodies of protein subunits of the ribonucleoprotein ribonuclease P. J Cell Biol 146:559–572.

Jones KW, Gorzynski K, Hales CM, Fischer U, Badbanchi F, Terns RM, Terns MP. 2001. Direct interaction of the spinal muscular atrophy disease protein SMN with the small nucleolar RNA-associated protein fibrillarin. J Biol Chem 276:38645–38651.

Kadowaki T, Schneiter R, Hitomi M, Tartakoff AM. 1995. Mutations in nucleolar proteins lead to nucleolar accumulation of polyA+ RNA in Saccharomyces cerevisiae. Mol Biol Cell 6:1103–1110.

Kressler D, Linder P, de La Cruz J. 1999. Protein transacting factors involved in ribosome biogenesis in Saccharomyces cerevisiae. Mol Cell Biol 19:7897–7912.

Lam YW, Lyon CE, Lamond AI. 2002. Large-scale isolation of Cajal bodies from HeLa cells. Mol Biol Cell 13:2461–2473.

Lamond AI, Earnshaw WC. 1998. Structure and function in the nucleus. Science 280:547–553.

Lefebvre S, Burlet P, Viollet L, Bertrandy S, Huber C, Belser C, Munnich A. 2002. A novel association of the SMN protein with two major non-ribosomal nucleolar proteins and its implication in spinal muscular atrophy. Hum Mol Genet 11:1017–1027.

Lengyel P. 1993. Tumor-suppressor genes: News about the interferon connection. Proceedings of the National Academy of Sciences of the United States of America 90:5893–5895.

Liu Q, Dreyfuss G. 1996. A novel nuclear structure containing the survival of motor neurons protein. Embo J 15:3555–3565.

Liu Q, Fischer U, Wang F, Dreyfuss G. 1997. The spinal muscular atrophy disease gene product, SMN, and its associated protein SIP1 are in a complex with spliceosomal snRNP proteins. Cell 90:1013–1021.

Liu CJ, Wang H, Lengyel P. 1999. The interferon-inducible nucleolar p204 protein binds the ribosomal RNA-specific UBF1 transcription factor and inhibits ribosomal RNA transcription. Embo J 18:2845–2854.

Lyon CE, Bohmann K, Sleeman J, Lamond AI. 1997. Inhibition of protein dephosphorylation results in the accumulation of splicing snRNPs and coiled bodies within the nucleolus. Exp Cell Res 230:84–93.

Massenet S, Pellizzoni L, Paushkin S, Mattaj IW, Dreyfuss G. 2002. The SMN complex is associated with snRNPs throughout their cytoplasmic assembly pathway. Mol Cell Biol 22:6533–6541.

Matera AG. 1999. Nuclear bodies: Multifaceted subdomains of the interchromatin space. Trends Cell Biol 9:302–309.

Matera AG, Frey MR. 1998. Coiled bodies and gems: Janus or gemini? Am J Hum Genet 63:317–321.

Matthews DA. 2001. Adenovirus protein V induces redistribution of nucleolin and B23 from nucleolus to cytoplasm. J Virol 75:1031–1038.

Maul GG, Negorev D, Bell P, Ishov AM. 2000. Review: Properties and assembly mechanisms of ND10, PML bodies, or PODs. J Struct Biol 129:278–287.

Meister G, Buhler D, Laggerbauer B, Zobawa M, Lottspeich F, Fischer U. 2000. Characterization of a nuclear 20S complex containing the survival of motor neurons (SMN) protein and a specific subset of spliceosomal Sm proteins. Hum Mol Genet 9:1977–1986.

Meurs E, Chong K, Galabru J, Thomas NS, Kerr IM, Williams BR, Hovanessian AG. 1990. Molecular cloning and characterization of the human double-stranded RNA-activated protein kinase induced by interferon. Cell 62:379–390.

Moser MJ, Holley WR, Chatterjee A, Mian IS. 1997. The proofreading domain of Escherichia coli DNA polymerase I and other DNA and/or RNA exonuclease domains. Nucleic Acids Res 25:5110–5118.

Narayanan A, Speckmann W, Terns R, Terns MP. 1999. Role of the box C/D motif in localization of small nucleolar RNAs to coiled bodies and nucleoli. Mol Biol Cell 10:2131–2147.

Narayanan U, Ospina JK, Frey MR, Hebert MD, Matera AG. 2002. SMN, the spinal muscular atrophy protein, forms a pre-import snRNP complex with snurportin1 and importin beta. Hum Mol Genet 11:1785–1795.

Negorev D, Maul GG. 2001. Cellular proteins localized at and interacting within ND10/PML nuclear bodies/PODs suggest functions of a nuclear depot. Oncogene 20:7234–7242.

Nguyen LH, Espert L, Mechti N, Wilson DM III. 2001. The human interferon- and estrogen-regulated ISG20/HEM45 gene product degrades single-stranded RNA and DNA in vitro. Biochemistry 40:7174–7179.

Ogg SC, Lamond AI. 2002. Cajal bodies and coilin–moving towards function. J Cell Biol 159:17–21.

Olson MO, Dundr M, Szebeni A. 2000. The nucleolus: An old factory with unexpected capabilities. Trends Cell Biol 10:189–196.

Pederson T. 1998. The plurifunctional nucleolus. Nucleic Acids Res 26:3871–3876.

Pellizzoni L, Baccon J, Charroux B, Dreyfuss G. 2001. The survival of motor neurons (SMN) protein interacts with the snoRNP proteins fibrillarin and GAR1. Curr Biol 11:1079–1088.

Platani M, Goldberg I, Swedlow JR, Lamond AI. 2000. In vivo analysis of Cajal body movement, separation, and joining in live human cells. J Cell Biol 151:1561–1574.

Player MR, Torrence PF. 1998. The 2-5A system: Modulation of viral and cellular processes through acceleration of RNA degradation. Pharmacol Ther 78:55–113.

Puvion-Dutilleul F, Mazan S, Nicoloso M, Pichard E, Bachellerie JP, Puvion E. 1992. Alterations of nucleolar ultrastructure and ribosome biogenesis by actinomycin D. Implications for U3 snRNP function. Eur J Cell Biol 58:149–162.

Raue HA, Planta RJ. 1991. Ribosome biogenesis in yeast. Prog Nucleic Acid Res Mol Biol 41:89–129.

Samarsky DA, Fournier MJ, Singer RH, Bertrand E. 1998. The snoRNA box C/D motif directs nucleolar targeting and also couples snoRNA synthesis and localization. Embo J 17:3747–3757.

Scheer U, Hock R. 1999. Structure and function of the nucleolus. Curr Opin Cell Biol 11:385–390.

Schneiter R, Kadowaki T, Tartakoff AM. 1995. mRNA transport in yeast: Time to reinvestigate the functions of the nucleolus. Mol Biol Cell 6:357–370.

Schofer C, Weipoltshammer K, Almeder M, Muller M, Wachtler F. 1996. Redistribution of ribosomal DNA after blocking of transcription induced by actinomycin D. Chromosome Res 4:384–391.

Shaw PJ, Jordan EG. 1995. The nucleolus. Annu Rev Cell Dev Biol 11:93–121.

Shpargel KB, Ospina JK, Tucker KE, Matera AG, Hebert MD. 2003. Control of Cajal body number is mediated by the coilin C-terminus. J Cell Sci 116:303–312.

Sleeman J, Lyon CE, Platani M, Kreivi JP, Lamond AI. 1998. Dynamic interactions between splicing snRNPs, coiled bodies and nucleoli revealed using snRNP protein fusions to the green fluorescent protein. Exp Cell Res 243:290–304.

Sleeman JE, Ajuh P, Lamond AI. 2001. snRNP protein expression enhances the formation of Cajal bodies containing p80-coilin and SMN. J Cell Sci 114:4407–4419.

Sleeman JE, Trinkle-Mulcahy L, Prescott AR, Ogg SC, Lamond AI. 2003. Cajal body proteins SMN and Coilin show differential dynamic behaviour in vivo. J Cell Sci 116:2039–2050.

Stark GR, Kerr IM, Williams BR, Silverman RH, Schreiber RD. 1998. How cells respond to interferons. Annu Rev Biochem 67:227–264.

Terns MP, Terns RM. 2001. Macromolecular complexes: SMN–the master assembler. Curr Biol 11:862–864.

Tollervey D, Kiss T. 1997. Function and synthesis of small nucleolar RNAs. Curr Opin Cell Biol 9:337–342.

Tourriere H, Chebli K, Tazi J. 2002. mRNA degradation machines in eukaryotic cells. Biochimie 84:821–837.

Tsukamoto T, Hashiguchi N, Janicki SM, Tumbar T, Belmont AS, Spector DL. 2000. Visualization of gene activity in living cells. Nat Cell Biol 2:871–878.

Tucker KE, Berciano MT, Jacobs EY, LePage DF, Shpargel KB, Rossire JJ, Chan EK, Lafarga M, Conlon RA, Matera AG. 2001. Residual Cajal bodies in coilin knockout mice fail to recruit Sm snRNPs and SMN, the spinal muscular atrophy gene product. J Cell Biol 154:293–307.

van Hoof A, Lennertz P, Parker R. 2000. Three conserved members of the RNase D family have unique and overlapping functions in the processing of 5S, 5.8S, U4, U5, RNase MRP and RNase P RNAs in yeast. Embo J 19:1357–1365.

Venema J, Tollervey D. 1996. RRP5 is required for formation of both 18S and 5.8S rRNA in yeast. Embo J 15:5701–5714.

Verheggen C, Lafontaine DL, Samarsky D, Mouaikel J, Blanchard JM, Bordonne R, Bertrand E. 2002. Mammalian and yeast U3 snoRNPs are matured in specific and related nuclear compartments. Embo J 21:2736–2745.

Wehner KA, Ayala L, Kim Y, Young PJ, Hosler BA, Lorson CL, Baserga SJ, Francis JW. 2002. Survival motor neuron protein in the nucleolus of mammalian neurons. Brain Res 945:160–173.

Williams BR. 2001. Signal integration via PKR. Sci STKE 2001:RE2.

Young PJ, Le TT, Dunckley M, Nguyen TM, Burghes AH, Morris GE. 2001. Nuclear gems and Cajal (coiled) bodies in fetal tissues: Nucleolar distribution of the spinal muscular atrophy protein, SMN. Exp Cell Res 265:252–261.

Zhou A, Hassel BA, Silverman RH. 1993. Expression cloning of 2-5A-dependent RNAase: A uniquely regulated mediator of interferon action. Cell 72:753–765.

Zuo Y, Deutscher MP. 2001. Exoribonuclease superfamilies: Structural analysis and phylogenetic distribution. Nucleic Acids Res 29:1017–1026.